คุณสมบัติทางด้านความแข็งแกร่งของการยึดเกาะของการเคลือบผิวที่มีโครงสร้างระดับนาโน

นุโรจน์ พานิช [1*] และ วีระศักดิ์ กรัยวิเชียร [2]

วิทยาลัยรัชต์ภาคย์ แขวงวังทองหลาง เขตวังทองหลาง กรุงเทพฯ 10310

รับเมื่อ 18 พฤษภาคม 2547 ตอบรับเมื่อ 19 มกราคม 2548

บทคัดย่อ

งานวิจัยนี้ได้เน้นการศึกษาคุณสมบัติทางด้านความแข็งแกร่งของการยึดเกาะของการเคลือบผิวแข็งเป็นพิเศษที่มีโครงสร้างระดับนาโน โดยการเคลือบด้วยไททาเนียมไดบอไรด์ การเคลือบผิวแข็งเป็นพิเศษที่มีโครงสร้างระดับนาโนนี้สร้างโดยเครื่องแมกนีตรอนสปัตเตอร์ริ่ง ส่วนการวิเคราะห์คุณสมบัติของความแข็งแกร่งของการยึดเกาะของการเคลือบผิวได้ใช้วิธีการขูดขีดระดับไมครอน งานวิจัยนี้มีการเพิ่มคุณสมบัติทางด้านความแข็งแกร่งของการยึดเกาะของการเคลือบผิว โดยการควบคุมปัจจัยตัวแปรในการเคลือบผิว เช่น กำลังไฟฟ้าที่ใช้ในการเคลือบ อุณหภูมิของชิ้นงานระหว่างเคลือบ และเวลาที่ใช้ในการเคลือบ และใช้เทคนิคการเคลือบแบบหลายชั้น โดยการเคลือบไททาเนียมไดบอไรด์ซึ่งเป็นวัสดุแข็งกับวัสดุที่มีความเหนียวมากกว่าได้แก่ ไททาเนียมและอะลูมินั่ม

คำสำคัญ : การเคลือบผิวด้วยไททาเนียมไดบอไรด์ / การขูดขีดระดับไมครอน / แมกนีตรอนสปัตเตอร์ริ่ง / การยึดเกาะ

---

[1] อาจารย์ สาขาวิชาวิศวกรรมเครื่องกล

[2] รองศาสตราจารย์ สาขาวิชาวิศวกรรมเครื่องกล

Characterisation of Adhesion Strength of Nano-structured Coatings

Nurot Panich [1*] and Virasak Kraivichien [2]

Rajapark College, Wangthonglang, Bangkok, 10310

Received 18 May 2004 ; accepted 19 January 2005

Abstract

This research focused on the characterisation of coating adhesion or adhesion strength of superhard coating, TiB_2-based nano-structured coatings. The nano-structured coating was fabricated using magnetron sputtering. Micro-scratch test was used to examine the coating adhesion and scratch resistance. Attempts to enhance the adhesion strength of TiB_2-based nano-structured coatings by controlling the deposition parameters, such as, sputter target power, substrate temperature, sputtering time are also presented. In addition, in order to enhance the coating adhesion, graded and multilayer techniques between TiB_2 and tough material, e.g. Ti and Al were also proposed and employed.

Keywords : Titanium Diboride Coating / Micro-scratch / Magnetron Sputtering / Adhesion

[1] *Lecturer, Department of Mechanical Engineering.*

[2] *Associate Professor, Department of Mechanical Engineering.*

[*] *Author for correspondence E-mail: panich@pmail.ntu.edu.sg.*

1. Introduction

Coatings are widely used in contemporary engineering applications, such as microelectronic, packaging, biomedical, decorative applications tool, machine parts and even impact resistant armor [1]. However, in order to achieve the functional behaviour of these coatings, mechanical properties and coating adhesion are critical. So far, superhard coatings in terms of mechanical properties can be achieved but not desired adhesion.

At present, there are many types of superhard materials, such as TiN, TiB_2, etc. However, in comparison to the well-known TiN, TiB_2 has a lower expansion coefficient, a better adhesion to metallic substrate, high melting point, high hardness value, and shows a good electrical conductivity. From these reasons, TiB_2-based coatings is one of the most widely studied hard material particularly for wear resistant applications [2-5]. It is also easy to fabricate employing various methods, for instance CVD [6], plasma spraying [7], electron beam vapourisation [8], magnetron sputtering [2], [9] and laser assisted techniques [10].

Since TiB_2-based coatings demonstrate the nano-structured materials, and most likely the coatings are designed to be thin in many applications, it is not easy to evaluate their properties by traditional approaches. Micro- testing method then was employed in this work i.e. micro-scratch test, to analyze the coating-substrate adhesion as well as deformation and failure behaviour of the coatings.

In the present work, attempts were made to enhance the adhesion of TiB_2-based nano-structured coatings on high speed steel substrates by controlling the deposition parameters such as sputter target power, substrate temperature, and sputtering time. In addition, this paper discusses the effect of these processing parameters on scratch resistance of the resultant coatings.

2. Experimental Methods

2.1 Substrate materials and preparation

High speed steel (SECO WKE45, Sweden) in fully hardened and tempered condition was chosen as a substrate in this study. HSS was cut into 12 mm x 12 mm x 3 mm pieces. The specimen's surface was prepared in order to eliminate the surface roughness by grinding and polishing and was then ultrasonically cleaned before charging into the deposition chamber.

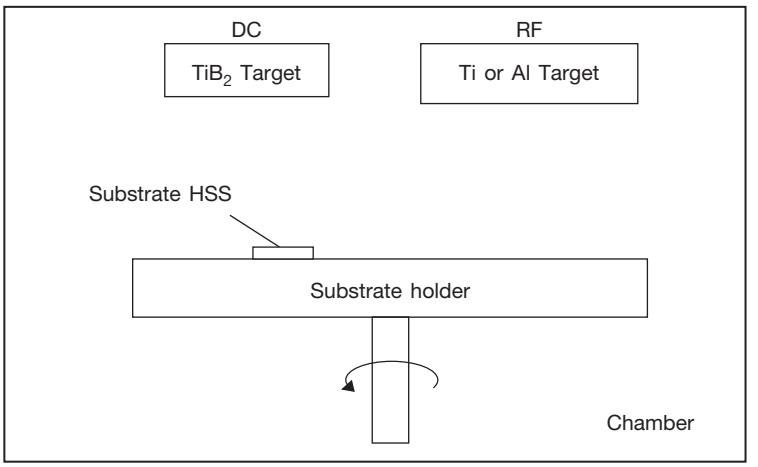

Fig. 1 Schematic diagram showing the co-sputtering process.

2.2 Nano-structured coating deposition

The MSS3 type planar magnetron sputtering system, manufactured by Coaxial Power System Ltd. (United Kingdom), was used to deposit TiB_2-based coatings. High-purity argon gas was introduced into the chamber after it was evacuated to below 5×10^{-4} Pa. The TiB_2 target was powered in the radio frequency (rf) mode and the Ti target was powered in the direct current (dc) mode as shown in Fig. 1. The targets were then pre-sputtered for 10 min with the target shutters closed. The working table was rotating at 6 rpm during the process. The substrate to target distance was held constant at 10 cm for DC target (Ti) and at 8 cm for RF target (TiB_2). All the experiments were conducted at a constant working pressure of 0.65 Pa and at a total gas flow rate (Ar) of 20 sccm (standard cubic centimeter). The substrate temperature was varied from room temperature (RT) to 400 °C. Table 3.2 summarises the various deposition conditions employed in this work. Table 1 summarises the various deposition conditions employed in this work and also the thickness of resultant coatings.

Table 1 Summary of deposition conditions for TiB_2 Coatings.

Materials	Mode	Substrate Temperature (°C)	Conditions	Coating Thickness (μm)
Sample 1	Graded Ti-TiB_2	RT	Ti 150 W 5 min, TiB_2 150 W 2 hours	0.40
Sample 2	Graded Ti-TiB_2	100	Ti 150 W 5 min, TiB_2 150 W 2 hours	0.40
Sample 3	Graded Ti-TiB_2	200	Ti 150 W 5 min, TiB_2 150 W 2 hours	0.40
Sample 4	Graded Ti-TiB_2	300	Ti 150 W 5 min, TiB_2 150 W 2 hours	0.45
Sample 5	Graded Ti-TiB_2	RT	Ti 300 W 5 min, TiB_2 300 W 2 hours	0.53
Sample 6	Graded Ti-TiB_2	100	Ti 300 W 5 min, TiB_2 300 W 2 hours	0.66
Sample 7	Graded Ti-TiB_2	200	Ti 300 W 5 min, TiB_2 300 W 2 hours	0.69
Sample 8	Graded Ti-TiB_2	300	Ti 300 W 5 min, TiB_2 300 W 2 hours	0.70
Sample 9	Graded Ti-TiB_2	400	Ti 350 W 20 min, TiB_2 350 W 3 hours	1.05
Sample 10	Multilayer Ti-TiB_2	400	Ti 200 W 20 min , TiB_2 350 W 1 hour & Ti 200 W 20 min, TiB_2 350 W 1 hour & Ti 200 W 20 min, TiB_2 350 W 1 hour	1.20
Sample 11	Multilayer Ti-TiB_2	400	Ti 200 W 20 min, TiB_2 350 W 1 hour & Ti 200 W 10 min, TiB_2 350 W 1 hour & Ti 200 W 10 min, TiB_2 350 W 1 hour &	1.08
Sample 12	Multilayer Ti-TiB_2	400	Ti 200 W 20 min, TiB_2 350 W 1 hour & Ti 200 W 5 min, TiB_2 350 W 1 hour & Ti 200 W 5 min, TiB_2 350 W 1 hour	1.00
Sample 13	Multilayer Al-TiB_2	400	Al 200 W 20 min, TiB_2 350 W 1 hour Al 200 W 20 min, TiB_2 350 W 1 hour & Al 200 W 20 min, TiB_2 350 W 1 hour	2.67
Sample 14	Multilayer Al-TiB_2	400	Al 200 W 20 min, TiB_2 350 W 1 hour & Al 200 W 10 min, TiB_2 350 W 1 hour & Al 200 W 10 min, TiB_2 350 W 1 hour	2.00
Sample 15	Multilayer Al-TiB_2	400	Al 200 W 20 min, TiB_2 350 W 1 hour & Al 200 W 5 min, TiB_2 350 W 1 hour & Al 200 W 5 min, TiB_2 350 W 1 hour	1.80

2.3 Energy Dispersive Spectroscopy (EDS)

Energy Dispersive Spectroscopy (EDS) analyses were also performed using a SEM, JEOL 5410LV. A focused beam of electrons was scanned across a sample surface and synchronized with the raster of a cathode ray tube. The secondary electrons or backscattered electrons produced were detected and used to adapt the brightness of the cathode ray tube. Since the electron beam also generates the emission of X-rays characteristic of the elements present, energy dispersive analysis of the X-rays provides a means of elemental identification.

2.4 Micro-scratch adhesion test

The micro-scratch test was performed using NanoTest™ device (Micro Materials Ltd., Wrexham, United Kingdom) with an indenter topped with a conical with spherical end form of 25 μm in radius. The stylus was moved tangential to the surface at speed 5 μm/s over a length of 550 μm. At the same time, the applied load was increased linearly at a rate of 5 mN/s from 0 to 500 mN. All scratch tests were performed at ambient temperature.

3. Results and Discussion

Fifteen TiB_2-based nano-structured coatings have been fabricated under various sputtering conditions, which allow for the evaluation of the effect of sputter target power, substrate temperature and sputtering time on the structures and properties of the resultant coatings, as evaluated by means of micro-scratch test. Three types of coatings have been fabricated as schematically illustrated in Fig. 2. These include:

(1) Graded Ti-TiB_2 coatings, by depositing a thin Ti interfacial layer at the interface followed by a TiB_2 layer on top (Fig. 2 (a)),

(2) Multilayer Ti-TiB_2 coatings, by depositing 6 alternate Ti and TiB_2 layers with varying Ti layer thickness (Fig. 2 (b)), and

(3) Multilayer Al-TiB_2 coatings, by depositing 6 alternate Al and TiB_2 layers with varying Al layer thickness (Fig. 2 (c)).

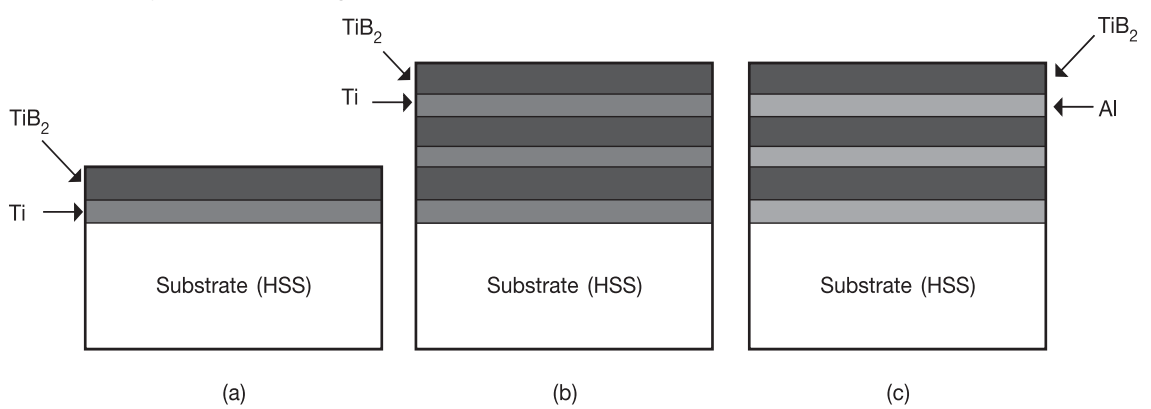

Fig. 2 Schematics of fabricated specimens:
(a) Graded Ti-TiB_2 coatings, (b) Multilayer Ti-TiB_2 coatings, and (c) Multilayer Al-TiB_2 coatings.

The morphology and thickness of the deposited coatings were examined under FESEM. The thickness values of the coatings are summerised in Table 1. All samples exhibit a columnar structure in the cross section. The size of the grains is in nanometer scale, typical less than 80 nm in all dimensions.

Coating adhesion was assessed using micro-scratch mode of the NanoTest™. Both L_{C1} and L_{C2} (critical loads for cohesive and adhesive failures, respectively) were determined from a scratch on each sample. L_{C2} was taken as the load at which the first exposure of the substrate could be identified, while L_{C1} was taken as the load at which failures within the coating started to occur. The simplest method for evaluation the critical load is to plot friction force vs load. Optical and scanning electron microscopic examinations were also used to confirm the results from the friction curve.

As expected, since samples 1 to 8 have a very thin coating thickness, cohesive failure (L_{C1}) could not be detected, but only adhesive failure could be found. The critical load, L_{C2}, for adhesive failure of all the graded coatings (samples 1 to 8), was found to be very low, in the range between 16 mN to 30 mN. No correlation has been found between L_{C2} and substrate temperature and sputtering power. Fig. 3 shows a typical plot of the friction force vs load (sample 8).

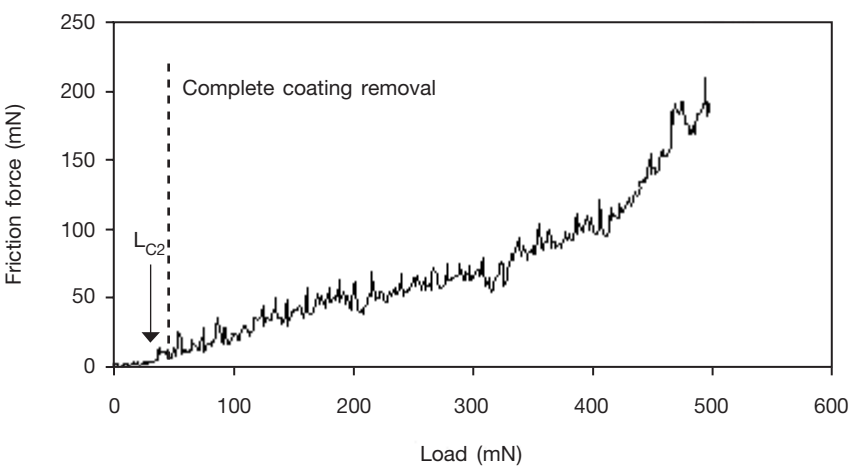

Fig. 3 Plot of the friction force vs load of sample 8.

From the experimental results, it can be seen that samples 1 to 8 had a very poor coating adhesion probably due to the brittle nature of TiB_2, the thin coating thickness and the absence of substrate biasing during depositions.

In order to confirm the result of scratch test, SEM images and EDS mapping images of the scratch track were acquired. SEM and mapping images reveal the adhesive failure behaviour of the coatings and allow for the measurement of the critical length corresponding to the critical load (L_{C2}). The results from SEM examinations agree with the results measured by friction force- load curves.

The graded Ti-TiB_2 system, sample 9, shows the interesting friction force-load curve as shown in Fig. 4, from which three zones can be defined, i.e. coating polished by indenter, coating break-down, and complete coating removal. In conjunction with microscopic examination, it was found that in sample 9, the graded Ti-TiB_2 coating was initially polished by the stylus until the film started to be removed at 65 mN (L_{C1}).

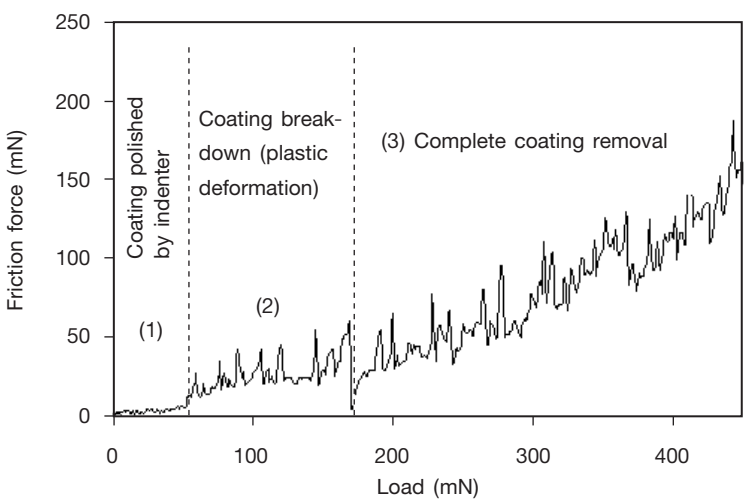

Fig. 4 Plot of the friction force vs load of sample 9.

With load increasing from 65 mN to 175 mN, plastic deformation occurred by causing the coating to break-down. Eventually the coating was removed completely when the load applied was more than 175 mN (L_{C2}). It is also noted that the adhesion of this graded Ti-TiB_2 coating was improved much as compared to samples 1 to 8. It seems that this result comes from the advantage of a thicker Ti layer and a thicker TiB_2 coating.

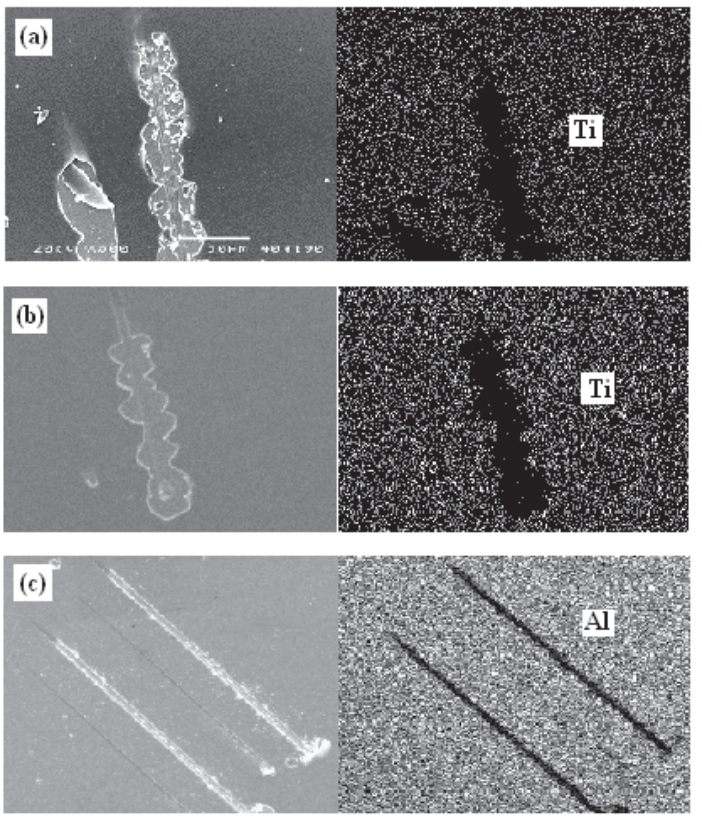

Fig. 5 SEM of damage region and EDX of the damage area illustrating (a) sample 9 (b) sample 10 and (c) sample 15.

Fig. 5 (a) shows that at the beginning of the scratch process, the film has not gone yet until the critical load, as confirmed by Ti mapping which shows the distribution of Ti (the white colour dots) in the scratch track and coating surface. Obviously, there is no remaining Ti in the scratch track after a certain critical scratch distance (load), which means that the film was already removed. In order to identify the failure modes of the coatings, the SEM images were further examined. From Fig. 5, it was found that compressive spallation occurs in most of the coating tested (e.g. sample 9 and 10) (Fig. 5 (a) and (b)), whilst gross spallation takes place in the Al-TiB_2 multilayer systems (e.g. sample 15) (Fig. 5 (c)).

It is interesting to note that for sample 15, an Al-TiB_2 multilayer coating, the failure mode is gross spallation. It can be pondered that the coating adhesion is very poor due to the soft Al alternate layers. The coating adhesion of the Al-TiB_2 multilayer systems is much lower than that of the Ti-TiB_2 multilayer systems, because the Ti film has excellent adhesion with almost all materials, whilst Al film has obviously poor adhesive property. Table 3 summarises the critical loads by scratch test and the mode of coating failure.

Table 3: Summary of the critical load by scratch test.

Material	Mode	L_{C1} (mN)	L_{C2} (mN)	Failure Mode
Sample 1	Grade Ti-TiB_2	None	20.8	Compressive spallation
Sample 2	Grade Ti-TiB_2	None	21.1	Compressive spallation
Sample 3	Grade Ti-TiB_2	None	26.5	Compressive spallation
Sample 4	Grade Ti-TiB_2	None	10.2	Compressive spallation
Sample 5	Grade Ti-TiB_2	None	20.1	Compressive spallation
Sample 6	Grade Ti-TiB_2	None	16.3	Compressive spallation
Sample 7	Grade Ti-TiB_2	None	17.0	Compressive spallation
Sample 8	Grade Ti-TiB_2	None	18.1	Compressive spallation
Sample 9	Grade Ti-TiB_2	65.0	175.0	Compressive spallation
Sample 10	Multilayer Ti-TiB_2	307.5	335.1	Compressive spallation
Sample 11	Multilayer Ti-TiB_2	136.2	160.4	Compressive spallation
Sample 12	Multilayer Ti-TiB_2	84.4	135.5	Compressive spallation
Sample 13	Multilayer Al-TiB_2	None	93.6	Gross spallation
Sample 14	Multilayer Al-TiB_2	None	71.6	Gross spallation
Sample 15	Multilayer Al-TiB_2	None	67.0	Gross spallation

From Table 3, it is noted that the Ti-TiB_2 multilayer systems have the highest values of critical load among all the systems investigated. In particular, sample 10 has the best performance, which demonstrated a critical load for cohesive (L_{C1}) and adhesive failures (L_{C2}) of 307.5 mN and 335.1 mN respectively. It is obvious that the high adhesion results from a thicker Ti alternate layer. Fig. 6 shows the plot of the friction force-load curve, illustrating the details of three zones during scratch test.

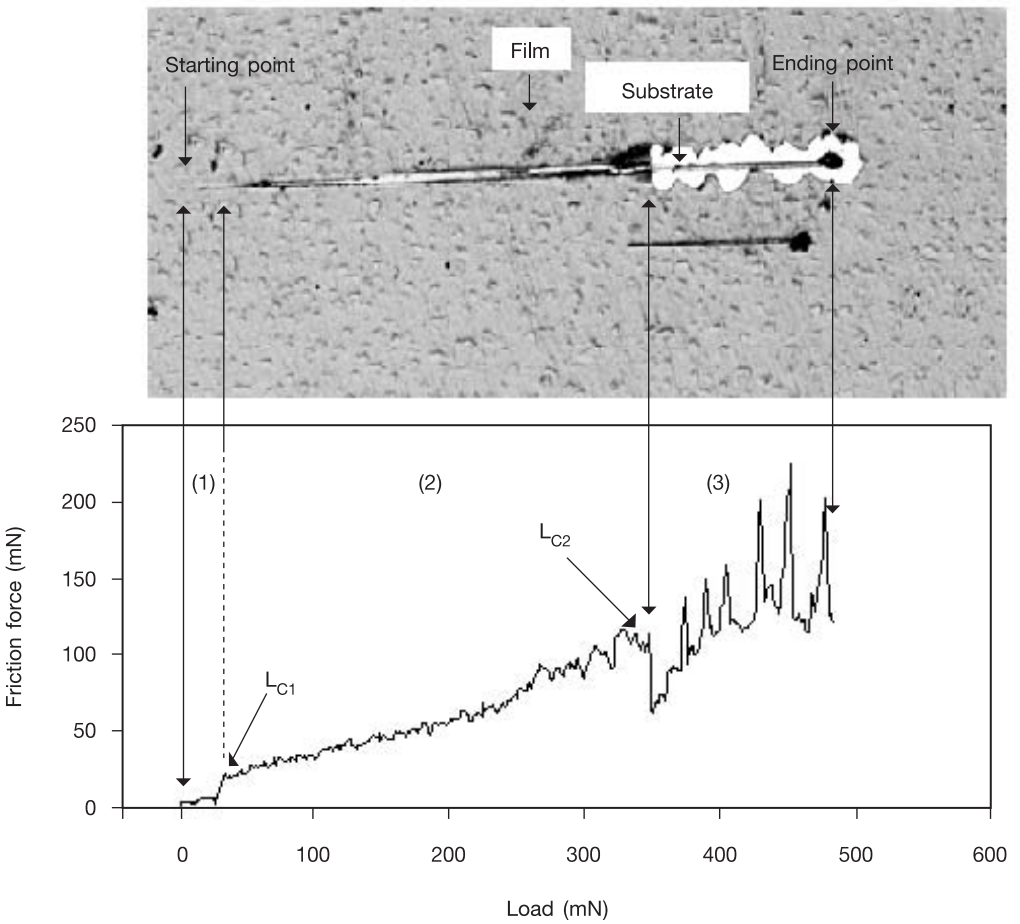

Fig. 6 Plot of friction force vs load for sample 10, with description for scratch test.

It can be seen that the polishing stage by the indenter is short, whilst the coating break-down or plastic deformation stage is long until reaching the complete coating removal point (L_{C2}). For the multilayer Al-TiB_2 systems, samples 13 to 15, there is no L_{C1} and the critical load for adhesive failure (L_{C2}) is much lower than the multilayer Ti-TiB_2 systems. From Fig. 7, it is obvious that the increase of the adhesion strength of the nanostructured TiB_2 coatings can be achieved by increasing the sputtering power, the deposition time and substrate temperature (Fig. 7 (a)). All the graded Ti-TiB_2 coatings show poor adhesion with the substrate, as revealed by the low L_{C2} values by scratch test. However, selected sample (sample 9) was chosen to show in Fig. 7 (b) due to the best performance among the graded one (Fig. 7 (b)). Fig. 7 (b) shows the comparison of critical load of the graded Ti-TiB_2 coatings,

Ti-TiB_2 multilayer systems and Al-TiB_2 multilayer systems, it can be seen that the adhesion strength of the coatings is much improved by introducing alternate layers of soft metals, such as Ti and Al. Furthermore the Ti-TiB_2 multilayer system exhibits the best adhesion strength (335.1 mN).

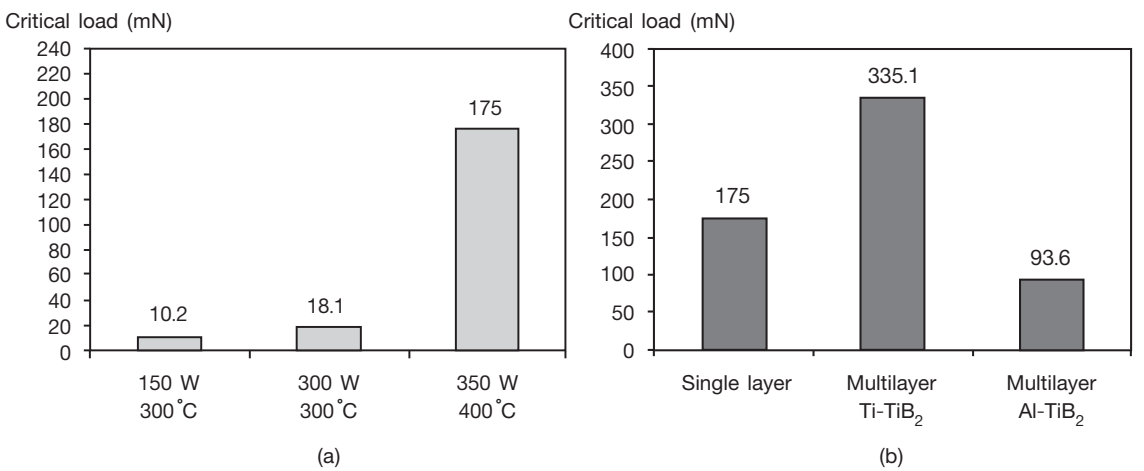

Fig. 7 Plot of critical load vs. (a) deposition parameters and (b) different system of coatings.

4. Conclusions

(1) Three types of TiB_2-based nanostructure coating systems have been fabricated by the magnetron sputtering techniques. These include Ti-TiB_2 graded coatings, multilayer Ti-TiB_2 coatings and multilayer Al-TiB_2 coatings.

(2) It was found that the increase of the adhesion strength of the nanostructured TiB_2 coatings may be achieved by increasing the sputtering power, the deposition time and substrate temperature.

(3) All the graded Ti-TiB_2 coatings show poor adhesion with the substrate, as revealed by the low L_{C2} values by scratch test. The adhesion strength of the coatings is much improved by introducing alternate layers of soft metals, such as Ti and Al. The Ti-TiB_2 multilayer system exhibits the best adhesion strength.

(4) For the graded Ti-TiB_2 system and multilayer Ti-TiB_2 system, all samples show the same failure mode during scratch test, which is compressive spallation, whilst gross spallation is shown for all samples of the multilayer Al-TiB_2 systems.

5. Acknowledgment

The authors would like to thank Prof. Dr. Y. Sun, School of Materials Engineering, Nanyang Technological University, Singapore, for the technical assistance.

6. References

1. Munro, R. G., 2000, "Material Properties of Titanium Diboride", *Journal of Research of the National Institute of Standards and Technology*, Vol. 105, pp. 709-720.

2. Matthes, B., Herr, W., and Broszeit , E., 1991, *Materials Science and Engineering A*, Vol. 140, p. 593.

3. Lee, K. W., Chen, Y. H., Chung, Y. W., and Keer, L. M., in press, "Hardness, Internal Stress and Thermal Stability of TiB_2/TiC Multilayer Coatings Synthesized by Magnetron Sputtering with and without Substrate Rotation", *Surface Coatings and Technology*.

4. Cutler, R. A., 1991, "Engineering Properties of Borides", *Engineering Materials Handbook: Ceramic and Glasses*, ASM International, Vol. 4, pp. 787-803.

5. Holleck, H. and Schier, V., 1995, "Multilayer PVD Coatings for Wear Protection", *Surface Coatings and Technology*, Vol. 76-77, pp. 328-336.

6. Berger, M., Karlsson, L., Larsson, M., and Hogmark, S., 2001, " Low Stress TiB_2 Coating with Improved Tribological Properties", *Thin Solid Film*, Vol. 401, pp. 179-186.

7. Treglio, J. R., Trujillo, S., and Perry, A. J., 1993, "Deposition of TiB_2 at Low Temperature with Low Residual Stress by a Vacuum Arc Plasma Source", *Surface and Coatings Technology*, Vol. 61, pp. 315-319.

8. Berger, M., Larsson, M., and Hogmark, S, 2000, "Evaluation of Magnetron-sputtered TiB_2 Intended for Tribological Application", *Surface and Coating Technology*, Vol. 124, pp. 253-261.

9. Berger, M., 2002, "Thick Physical Vapour Deposition TiB_2 Coatings", *Surface Engineering*, Vol. 18, No. 3, pp. 219-223.

10. Wiedemann, R., Weihnacht, V. H., and Oettel, H., 1999, "Structure and Mechanical Properties of Amorphous Ti-B-N Coatings", *Surface and Coatings Technology*, Vol. 116-119, pp. 302-309.